

Sub-milliarcsec-scale structure of the gravitational lens B1600+434

Alok R. Patnaik¹ and Athol J. Kemball²

¹ Max-Planck-Institut für Radioastronomie, Auf dem Hügel 69, D-53121 Bonn, Germany
e-mail: apatnaik@mpifr-bonn.mpg.de

² National Radio Astronomy Observatory, PO Box 0, Socorro, NM 87801, USA
e-mail: akemball@nrao.edu

Received date / Accepted date

Abstract. In the gravitational lens system B1600+434 the brighter image, A, is known to show rapid variability which is not detected in the weaker image, B (Koopmans & de Bruyn 2000). Since correlated variability is one of the fundamental properties of gravitational lensing, it has been proposed that image A is microlensed by stars in the halo of the lensing galaxy (Koopmans & de Bruyn 2000). We present VLBA observations of B1600+434 at 15 GHz with a resolution of 0.5 milliarcsec to determine the source structure at high spatial resolution. The surface brightness of the images are significantly different, with image A being more compact. This is in apparent contradiction with the required property of gravitational lensing that surface brightness be preserved. Our results suggest that both the lensed images may show two-sided elongation at this resolution, a morphology which does not necessarily favour superluminal motion. Instead these data may suggest that image B is scatter-broadened at the lens so that its size is larger than that of A, and hence scintillates less than image A.

Key words. Gravitational lensing – (Galaxies:) quasars: individual: B1600+434 – Radio continuum: galaxies

1. Introduction

The gravitational lens B1600+434 was discovered by Jackson et al. (1995). The radio source is a quasar at $z = 1.59$ and has two images separated by 1.4 arcsec, which are denoted A and B. The main lensing galaxy is identified as an edge-on spiral at $z = 0.41$, with an additional lensing contribution from a nearby companion galaxy (Jaunsen & Hjorth 1997, Fassnacht & Cohen 1998, Koopmans, de Bruyn & Jackson 1998). The background quasar is variable in both optical and radio bands, thus allowing time delay measurements from monitoring observations (Jaunsen & Hjorth 1997, Koopmans et al. 2000). A time delay of 47_{-9}^{+12} days has been determined from the radio monitoring (Koopmans et al. 2000), and a delay of 51 ± 4 days from the optical observations (Burud et al. 2000).

The radio observations of Koopmans et al. (2000) showed that the brighter image, A, varied more rapidly than the weaker image, B. The rapid variability in A was not found to be correlated with corresponding rapid variability in B, although differential variability between A and B on longer time scales allowed the measurement of the time delay mentioned above. Correlated variability is one of the fundamental characteristics of gravitational

lensing. Additional variability in A can only be explained by invoking propagation effects which affect image A only (Koopmans & de Bruyn 2000; hereinafter KdB). Such effects include a combination of scattering in the lensing galaxy and scintillation in our own galaxy, or microlensing in the halo of the lensing galaxy. KdB considered the possibility that B might be scatter-broadened in the lens and thereby would scintillate less than A. They argued however that the time scale and the frequency dependence of the variability, taken in conjunction with the high scattering measure required in the lens galaxy, did not favour scintillation as a possible cause. Instead, they proposed microlensing of image A in the halo of the lensing galaxy as a preferred alternative if the radio source has a superluminal component.

One of the ways to test these scenarios is to image the structure in the lensed images at high spatial resolution, and to apply the constraints imposed by gravitational lensing. In particular, the surface brightness of gravitationally lensed images must be equal and any significant departure would suggest that one of the images has been affected by scattering more than the other. Since the microlensing hypothesis requires the background quasar be a superluminal source, the images, therefore, might be expected to show evidence of this motion in their morphology, such as a core-jet structure typical of such quasars.

In addition, the polarization properties of the images can differ if one of the ray paths is affected either by scattering or microlensing.

With the above aims in mind, we observed B1600+434 at 15 GHz using the VLBA with a resolution of 0.5 milliarcsec (mas), to determine the fine-scale structure and to measure image sizes for A and B. The observations are described in Section 2 and the results are discussed in Section 3.

2. Observations and data analysis

We observed B1600+434 on 2000 September 9/10 (1900 UT to 0500 UT) at 15 GHz using all ten telescopes of the VLBA. The data were recorded in eight 8-MHz channels in dual circular polarization, yielding a total recorded bandwidth of 32-MHz per polarization. Two-bit sampling quantization was used. A single correlation centre was selected at $\alpha = 16^h 01^m 40.47^s$, $\delta = 43^d 16^m 47.2^s$ (J2000). Since the image separation of 1.4 arcsec is large compared with the resolution of 0.5 mas, it is necessary to sample the data finely both in frequency and time to avoid smearing of the visibility function and the associated image distortions in the field of view. The data were therefore sampled at 0.5 MHz in frequency and 0.5 sec in time.

We observed 3C345 (J1640+3946), 1611+343 (J1613+3412) and 1749+096 (J1751+0939) as calibrators. The total integration time on the target source B1600+434 was 195 min. We used 1749+096 to calibrate the instrumental polarization, as well as to determine the bandpass function.

The method of data analysis follows closely that described by Patnaik et al. (1999) as used for the gravitational lens B1422+231. The data were analysed using the software package AIPS, maintained by the National Radio Astronomy Observatory (NRAO). After correcting for the parallactic angle variation of the telescopes, amplitudes were calibrated using the system temperatures and telescope gain factors as a function of elevation. The phase slopes and offsets across each 8-MHz band were aligned using the pulse-cal information from each telescope. Standard fringe-fitting was performed on the calibrators. After careful editing, the bandpass function was determined using the source 1749+096. We followed the usual procedure for calibrating instrumental polarization, using 1749+096 as the polarization calibrator. Typical instrumental polarization amplitude was measured to be $\sim 1.6\%$. Since B1600+434 has two images with similar flux densities at a large angular separation, we had to iterate the fringe-fitting process several times, each time using the model of the source determined from the previous solution.

The final map was made with two sub-fields, centred on each lensed image. We also made polarization maps of the source in Stokes I , Q and U .

Image	Peak in mJy/beam	Total in mJy	Size mas \times mas, PA
A	9.0 \pm 0.15	17.2 \pm 0.5	0.69 \times 0.25, 103 $^\circ$
B	6.6 \pm 0.15	13.5 \pm 0.5	0.73 \times 0.30, 93 $^\circ$

Table 1. Peak (in mJy/beam) and total (in mJy) flux densities of the lensed images of B1600+434 at 15 GHz. The image deconvolved sizes were obtained by fitting a single gaussian in the program JMFIT. The error in the measured size is 0.01 mas in each axis for image A and about 0.015 mas for image B, and 1° in position angle. The image separation of B from A is 723.08 ± 0.05 mas to the east (in RA) and 1189.16 ± 0.05 mas to the south (in Dec).

3. Results and Discussion

The maps of the lensed images, made using uniform weighting, are shown in Fig.1. The maps have been restored using a circular gaussian with a FWHM of 0.5 mas. We did not detect any polarized emission from either component A or B, yielding a 5σ limit to the percentage linear polarization of 2.6% for image A, and 3.3% for image B. The rms noise in the polarization map is 0.09 mJy/beam.

Table 1 lists the results of fitting a single gaussian component to each of the images. Two clear results emerge from these observations. First, both the images are resolved, and A is more compact than B. Secondly, the structure is elongated on either side of the peak in both of the images. In order to quantify the errors of the size measurements we divided the data into two sets by removing alternate scans so as to preserve similar uv-coverage. The resulting maps were then fitted with a single gaussian. The results show that the errors for image A are ~ 0.01 mas in each axis. However, the errors are larger for image B by about 50%. Note that the error estimates derived in this way fold in most systematic calibration or imaging errors which may affect the component size measurement, excluding deviation of the component from non-Gaussian shape. A weak extension is seen to the south of image B which appears to be genuine as it is present in both the datasets mentioned earlier. We are not entirely certain if it is real as there is no counterpart in image A. This can be confirmed by another independent dataset. The measured size of image B, however, is not affected by including this feature.

The implication of the first result is that the surface brightnesses of the two images differ significantly. The flux density ratio of A/B is 1.27 ± 0.05 whereas the ratio of image sizes is 0.80 ± 0.15 . Secondly, the image morphology as measured is in apparent conflict with a typical superluminal radio source in the sense that such radio sources are core-dominated and must have one-sided jets due to relativistic motion Doppler boosting of the knot components.

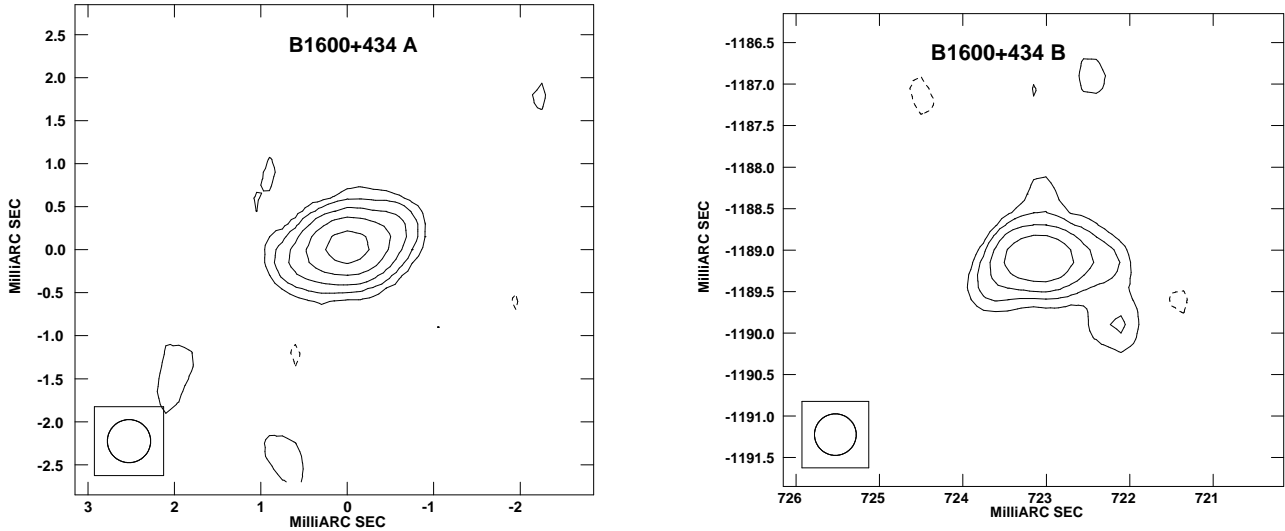


Fig. 1. 15 GHz map of B1600+434 A (left) and B (right). The contour levels for both the images are $-2, -1, 1, 2, 4, 8, 16, 32, 64, 128 \times$ the contour interval which is chosen as the 3σ noise in the map. For image A, contour interval is $0.42 \text{ mJy beam}^{-1}$ and peak flux density is $9.5 \text{ mJy beam}^{-1}$ and for image B contour interval is $0.42 \text{ mJy beam}^{-1}$ and the peak is $6.7 \text{ mJy beam}^{-1}$. The convolving beam of 0.5 mas circular gaussian is drawn at the lower left-hand corner in each map.

In order to understand the higher modulation index (fractional rms variability) of image A (2.8% at 8.4 GHz), KdB considered the possibility that the size of B (modulation index of 1.6% at 8.4 GHz) might be larger through scatter-broadening by the ionised interstellar medium in the lens galaxy. The fact that the surface brightnesses do not agree, and in particular, that the weaker image B is more extended, suggests that B has been affected by propagation through the lensing galaxy more than A. This would support the idea that B is somewhat broadened by scattering in the lensing galaxy. We note that its ray path passes close to the bulge of this edge-on spiral galaxy whereas the ray path of A goes through the halo of the lens. For the two images to scintillate in our Galaxy, the required sizes are $62 \mu\text{arcsec}$ and $108 \mu\text{arcsec}$ for A and B respectively (KdB). Our observations cannot resolve such sizes and our measured sizes are considerably larger than these. We note, however, that the observed images have been parametrised as single gaussian components. This does not exclude any sub-structure in the source. Therefore, our result that image B is larger in size than image A is in general agreement with the expectation from scintillation taking place in our Galaxy.

KdB measured a modulation index $\leq 1.2\%$ at 1.4 GHz and 3.7% at 5 GHz. If the variability was due to scintillation, then the modulation index should have increased going to lower frequencies. However, if there is frequency-dependent structure then the modulation index can be smaller at lower frequencies. A flat spectrum source likely consists of more than one self-absorbed component (Cotton et al.1980). It is then possible that the compo-

nent which is compact and scintillates at 5.0 GHz, which may for example be the core, does not contribute much to the flux density at 1.4 GHz due to self-absorption. Some other component in the jet might be brighter at 1.4 GHz but this component would be more extended and therefore unlikely to scintillate. Therefore, a smaller modulation index at a lower frequency does not necessarily rule out scintillation occurring at a higher frequency. Such frequency-dependent structure has been noted in the gravitational lens B0218+357 (Patnaik & Porcas 1999).

The alternative explanation proposed by KdB is that A is microlensed in the halo of the lensing galaxy. However, for the microlensing to match the time-scale of variability, the model used by KdB requires that the background source be a superluminal source with a knot the size of a few μarcsec containing $\sim 5-11\%$ of the flux density, moving at an apparent speed in the range $\sim 9-26c$. The morphology of a superluminal source will of necessity be that of a bright core and one-sided jet, due to Doppler boosting of a relativistically moving knots in the jet. The detection of extensions on either side of the peak in both the lensed images here is contrary to the above expectation. It would, therefore, appear that superluminal motion in the background source is not favoured and hence the microlensing caustic crossing time will be much longer than the observed variability. However, it is also possible that the peak we observe is not necessarily the core; it might be a bright knot and thus still allow the possibility that the source could be intrinsically one-sided. We do not have sufficient resolution to distinguish this level of detailed structure. If we assume that the peak corresponds to the

core, which may be a reasonable assumption given the fact that these observations are at 15 GHz and with 0.5 mas resolution where cores usually brighter than knots, then it would imply that microlensing combined with superluminal motion in the background source may not be a viable explanation for the rapid variability of the lensed image A.

As an example, the two brightest images in the lens system B1422+231 have elongation produced by lensing (Patnaik & Porcas 1998, Patnaik et al. 1999). In this lens system the background radio source is also a flat spectrum object and at milliarcsec-scales does not have the standard core-jet structure. It has been suggested that the magnification in this source might be very high and that the background object could possibly be a radio-quiet object. A similar scenario is possible for B1600+434. Certainly, in both B1422+231 and B1600+434, no jet has been detected and both sources show two-sided emission. If the extension of the images we detect is due to stretching of the extended background emission by gravitational lensing, then we cannot be sure of the direction of the jet. However, should there be superluminal motion (which can be as much as 0.15 milliarcsec per year for the bright quasars), we would detect changes in image size after a year or two.

4. Conclusions

We have observed the gravitational lens system B1600+434 at 15 GHz using the VLBA at a resolution of 0.5 milliarcsec. We find that the two lensed images are resolved and have elongation on either side of the peak, and that the surface brightnesses of the images are significantly different. The image shapes do not appear to favour superluminal motion in the background radio source and hence the interpretation that A is microlensed is not favoured by these observations at this epoch. Our results are consistent with the view that image B is perhaps scatter-broadened by the interstellar medium of the lens galaxy, and therefore scintillates less than image A in our Galaxy. However, VLBI observations of the source at a range of other observing frequencies are required to provide further insight into this question.

Acknowledgements. We thank Peter Schneider for helpful discussion and J. Schmid-Burgk and Karl Menten for a careful reading of the manuscript. We would like to thank the referee A.G. de Bruyn for critical comments and helpful advice. The National Radio Astronomy Observatory is a facility of the National Science Foundation operated under cooperative agreement by Associated Universities, Inc.

References

Burud, I., Hjorth, J., Jaunsen, A.O., Andersen, M.I., Korhonen, H., Clasen, J.W., Pelt, J., Pijpers, F.P., Magain, P., Østensen, R. 2000, *ApJ*, 544, 117
 Cotton, W.D., Wittels, J.J., Shapiro, I.I., Marcaide, J., Owen, F.N., Spangler, S.R., Rius, A., Angulo, C., Clark, T.A., Knight, C.A. 1980, *ApJ*, 238, 123

Fassnacht, C.D., Cohen, J.G. 1998, *AJ*, 115, 377
 Jackson, N., de Bruyn, A.G., Myers, S., Bremer, M.N., Miley, G.K., Schilizzi, R.T., Browne, I.W.A., Nair, S., Wilkinson, P.N., Blandford, R.D., Pearson, T.J., Readhead, A.C.S. 1995, *MNRAS*, 274, L25
 Jaunsen, A.O., Hjorth, J. 1997, *A&A*, 317, L39
 Koopmans, L.V.E., de Bruyn, A.G. 2000, *A&A*, 358, 793
 Koopmans, L.V.E., de Bruyn, A.G., Jackson, N. 1998, *MNRAS*, 295, 534
 Koopmans, L.V.E., de Bruyn, A.G., Xanthopoulos, E., Fassnacht, C.D. 2000, *A&A*, 356, 391
 Patnaik, A.R., Kemball, A.J., Porcas, R.W., Garrett, M.A. 1999, *MNRAS*, 307, L1
 Patnaik, A.R., Porcas, R.W. 1998, in *Radio Emission from Galactic and Extragalactic Compact Sources*, ed. J.A. Zensus, G.B. Taylor & J.M. Wrobel (IAU Colloquium 164), ASP Conference Series 144, p319
 Patnaik, A.R., Porcas, R.W. 1999, in *Highly Redshifted Radio Lines*, ed. C.L. Carilli, S.J.E. Radford, K.M. Menten, G.I. Langston, ASP Conference Series 156, p247